Analysis of a Current Biased Eight-Pole Radial Active Magnetic Bearing Regarding Self-Sensing

Matthias Hofer, Dominik Wimmer, Manfred Schrödl

Technische Universität Wien, Gußhausstraße 25-29, A-1040 Vienna, Austria, matthias.hofer@tuwien.ac.at

***Abstract*— In this work a current biased radial active magnetic bearing is investigated with regard to a possible self-sensing operation. The bearing is designed by the help of finite element methods. The force characteristic is investigated and bearing parameters are identified by simulation. Additionally, the position dependency of the coil inductances is evaluated which is the basis for self-sensing. The fundamental principle of the rotor position determination based on current slopes by using the differential open loop transformers approach is presented. Further, simulations are performed to analyze AMB current signals with regard to the rotor position. Finally, experimental tests with an AMB prototype are shown to verify the theoretical analysis. The measured rotor position at constant eccentricity confirms the functionality and represents the starting point for a future implementation of the self-sensing control to the prototype and detailed analysis of the self-sensing performance.**

INTRODUCTION

Active Magnetic Bearings (AMB) are usually applied to high speed drives because of low losses, low maintenance and an operation without mechanical wear and/or under special environmental conditions. For simplification of AMB systems, instead of implementing position sensors for feedback control, self-sensing methods are field of research since many years [1,2]. Thus, the AMBs work as actuators and sensing-units simultaneously. This common functionality is advantageous to build compact bearings with low costs. In addition, by coincidence of the axial sensor and actuator location, problems in the AMB control regarding phase shifts at bending modes are avoided. In [3] so called sensorless or self-sensing technology was already investigated for homopolar permanent magnet biased three phase AMBs. Herein, the inductance of the AMB coil itself is evaluated depending on the rotor eccentricity by the derivative of the coil current. As stated in this work, a high self-sensing bandwidth was achieved, because the rotor position detection principle is included in the inverter pulse pattern and works with the inverter switching frequency. Even a self-sensing accuracy competitive to industrial position sensors was reached. Further, the differential current slope evaluation of opposite bearing coils reduces the influence of eddy currents and saturation.

Active magnetic bearings usually use a pre-magnetization to increase the so called force current factors K_I. At permanent magnet biased AMBs the pre-magnetization is generated by the permanent magnets and superimposed to the control flux generated by the AMB coils. Hence, losses for bias flux generation during the operation are avoided, but the bias flux remains constant and cannot be varied. Therefore, in this work the bias flux is excited by coils instead of permanent magnets. This allows an adjustment of the bias flux and a detailed investigation of the bias flux level with regard to self-sensing. In practical AMB applications the differential driving topology is often used. Here, two opposite coils carry the same bias current superimposed to a contrary control current. The advantage is that a low number of coils is implemented in the bearing. In contrast, at the differential winding topology the control winding and the bias winding are separated. Definitely, on the one hand for the bias coil excitation an appropriate power unit has to be implemented in the inverter, but on the other hand the opposite coils for differential evaluation of the rotor position are powered together by only one power unit. Finally, for the proposed AMB topology three H-bridges are used for driving a current biased radial AMB.

In the following section the eight-pole AMB design with a differential winding architecture and its parameters are presented. Further, the self-sensing principle by differential evaluation of current slopes is discussed. Finally, first experimental results of the AMB prototype with regard to sensorless rotor position detection are presented.

MAGNETIC BEARING DESIGN

Radial magnetic bearings are able to actively stabilize two DOFs (degrees of freedom) of a levitating rotor. Therefore, the five DOF control is usually realized by two radial and one axial AMBs. The radial AMB applies electromagnetic forces in two perpendicular directions to the rotor nearly independently from each other. For each axis the forces have to be applied in positive and negative directions. Therefore, two electro-magnets are working together in opposite direction. Thus, for the radial AMB four electromagnets are used in the classical arrangement. This arrangement was chosen in this work and the cross-section is presented in Fig. 1. Each C-core type electromagnet generates a North-(N) and South-pole (S) and is equipped with a bias and a control coil on every pole. For production and assembly reasons the four C-cores are connected by a common yoke. The winding configuration generates magnetic pole orientation with NNSSNNSS. All eight bias coils are connected in series. Consequently, iron losses at high rotational speeds are expected to be lower than using an alternating arrangement NSNSNSNS because of a lower magnetization frequency in the rotor. Thus, a heteropolar bearing arrangement is given which has a simple architecture. In contrast to homopolar bearings, where the three-dimensional magnetic flux path may require expensive materials and complex parts like sintered soft magnetic composites, the heteropolar arrangement can be

built by common electrical lamination stacks as usually used in rotating electrical machines. In addition to the costs of the permanent magnets, structural cost by the AMB stator are also higher. Therefore, the bearing costs of PM-biased homopolar AMBs are much higher than heteropolar current biased bearings.

The bearing geometry is designed and investigated by a 2D-Finite Element Analysis (FEA). The bearing shall be equipped to a high speed synchronous reluctance drive prototype. The stationary load caused by the rotor's gravity force at a horizontal shaft arrangement is only F_G=4N for each radial AMB. However, to ensure stable operation at high speeds covering forces related to rotor dynamic effects, the maximum achievable bearing forces have to be much higher. The current biased AMB provides the advantage for adjustment of the bearing to the required system performance. In Fig. 1 the flux path of the AMB is shown at currents I_{bias}=I_X =1A. In *y*-direction no control current is applied and only the bias flux is excited. Therefore, at centered rotor position no force component F_Y occurs. In *x*-direction a bias current as well as a control current are applied. Because of the same number of winding turns at the bias and control windings the flux is fully vanished at the lower poles. At the upper side the ampere-turns of both coils are superimposed and lead to a high flux density and a high force respectively. Because of the differential arrangement, at the lower coil the force gets reduced from the bias flux and simultaneously increased at the upper coil. Two opposite control coils are connected. Instead of an anti-serial connection an anti-parallel connection is used as also shown in Fig 5. This connection type is advantageous for a differential current slope evaluation as later will be shown.

For detailed analysis of the AMB, first the force characteristic and second, the inductance behavior with respect to the rotor position is discussed.

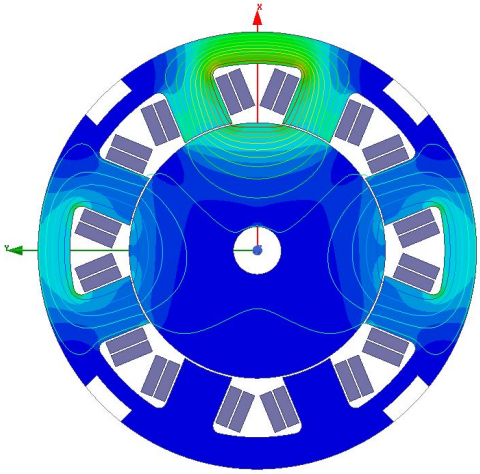

Figure 1. Finite element model and DC analyis of the flux paths at I_{bias} = 1A and I_X =1A.

A. *Force Analysis*

Active magnetic bearings are usually operated at a centered rotor position. Even for stabilization in the center as well as for any non-centered rotor operation the force characteristic related to a displacement and current excitation is of great significance. Therefore, the linearized force characteristic

$$F_X(x, I_X) = K_X\ x + K_I\ I_X \qquad (1)$$

with the coefficients K_X and K_I is used. For the perpendicular axis a characteristic $F_Y(y,I_Y)$ is used in the same manner. Usually, because of linearization a linear control approach is implemented for stabilization.

The differential coil arrangement is able to provide forces in both directions. By the combination of the bias coils and control coils at each pole, depending on the direction of I_X the flux is increased or decreased accordingly. By this arrangement, the opposite coil acts contrary. Thus, the sign of I_X is related to the force direction. In Fig. 2 the simulated force-current characteristic by the 2D-FEA is depicted.

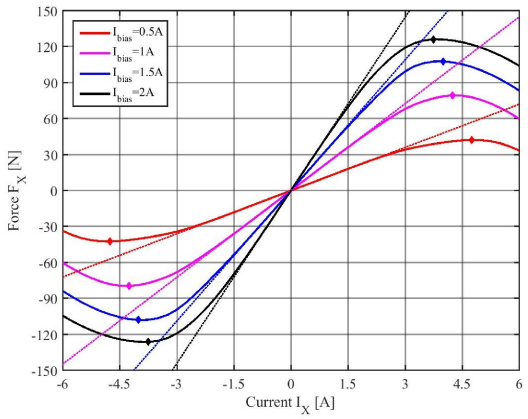

Figure 2. Simulation of the force-current characteristic at centered rotor and various bias currents I_{bias}, linearization with coefficient K_I (dotted) and maximum forces.

The force-current coefficient K_I represents the linearized parameter for control design and K_I increases by higher bias currents I_{bias} as also stated in Table I.

TABLE I. FORCE-CURRENT COEFFICIENTS AT VARIOUS BIAS CURRENTS AND CENTERED ROTOR

Bias Current I_{bias}	Coefficient K_I	Max. Force $F_{X,max}$
0.5A	12.00N/A	42.3N
1A	24.13N/A	79.5N
1.5A	36.30N/A	107.8N
2A	48.10N/A	126.2N

According to Fig. 2 the linear range of the actuator depends on the bias current level. At a bias current of I_{bias}=0.5A a linear range of approx. ±30N and a maximum force of 42.3N is given. At a higher bias current I_{bias}=2A the linear range is approx. ±60N at a maximum force 126.2N. These forces are much higher than the required stationary load from the rotor gravity force of F_G=4N for each bearing. Thus, depending on the bias current, the required force margin to handle rotor dynamic forces in operation at high speeds can be adjusted in a certain range. Further, the current biased AMB has a degree of freedom for optimization regarding a certain

parameter, e.g. with the target of loss minimization. In case of I_{bias}=0.5A the stationary control current to apply F_G to the rotor is I_X=0.333A and for I_{bias}=2A only I_X=0,083A is required. Applying very high control currents I_X to the bearing does not certainly lead to a further force increase (see Fig. 2). Because of saturation the maximum force for one pole is limited. At the opposite coil the counter acting force is not saturated because of the opposite bias current direction. Thus, to avoid any unstable operation the knowledge of the maximum force is of great importance for AMBs (see Tab. 1).

At non-centered rotor the force characteristic changes, e.g. as shown in Fig. 3 for a bias current I_{bias}=2A. In the force equation (1) this is covered by the coefficient K_X. An analysis of the eccentric rotor position at I_X=0 is shown in Fig. 4. For a displaced rotor the AMB generates a magnetic force which pushes the rotor to the safety bearings. At x>0 positive forces occur and for x<0 the magnetic forces have a negative sign. Depending on the bias current I_{bias} these destabilizing forces increase. By linearization around the centered rotor the so called force displacement coefficients are identified (see dotted lines in Fig. 4). The parameters are stated in Table II. Similar to the values K_I the coefficients K_X get higher by increasing bias current. Further, from this analysis (Fig. 4) the forces to lift up the rotor from the safety bearings are identified. In addition to the gravity force at I_{bias}=0.5A the rotor is pushed with force a F_X=-8.4N to the negative position limit x=-03mm. For a rotor movement in positive direction a higher force than F_G-F_X=12.4N has to applied by the electromagnets. At I_{bias}=2.0A this destabilizing force is even F_X=-100.8N.

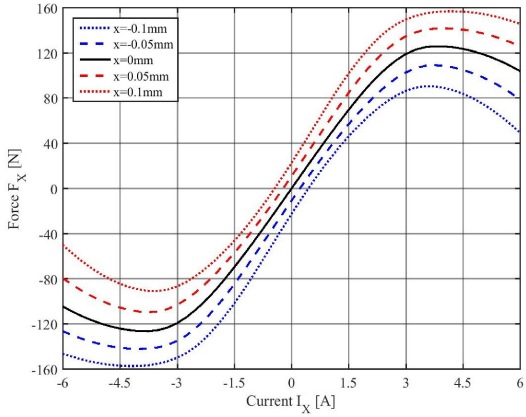

Figure 3. Simulation of the force-current characteristic at bias current I_{bias}=2A and at several displacements x.

B. *Inductance Analysis*

The coil inductances are of special interest for the realization of self-sensing or sensorless operation. For the classical arrangement with perpendicular coil axes the x,y-coordinate system coincides with the coil directions (Fig. 1). Two opposite C-cores and appropriate coils are related to the x- and the others to the y-axis. This structure allows the combination of two opposite coil inductances for a rotor position evaluation. The characteristic of two opposite coils obtained by a 2D-FEA is shown in Fig. 5. At positive displacements x the inductance $L_{X,top}$ increases because of a smaller airgap. In contrast, $L_{X,bot}$ at the bottom side decreases because of a higher airgap. At centered rotor x=0 both inductances are equal.

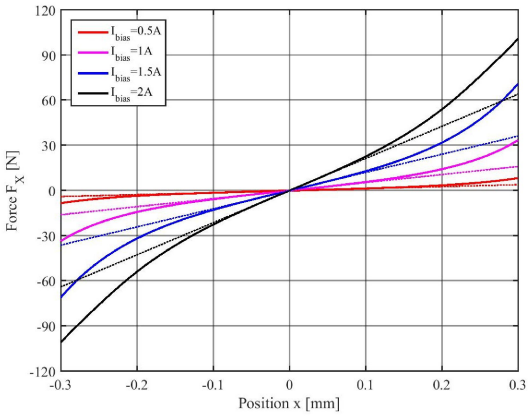

Figure 4. Simulation of the force-displacement characteristic at several bias currents and at I_X=0, linearization with coefficients K_X (dotted).

TABLE II. FORCE-DISPLACEMENT COEFFICIENTS AT VARIOUS BIAS CURRENTS

Bias Current I_{bias}	Coefficient K_X
0.5A	13.2N/mm
1A	53.4N/mm
1.5A	120.7N/mm
2A	213.3N/mm

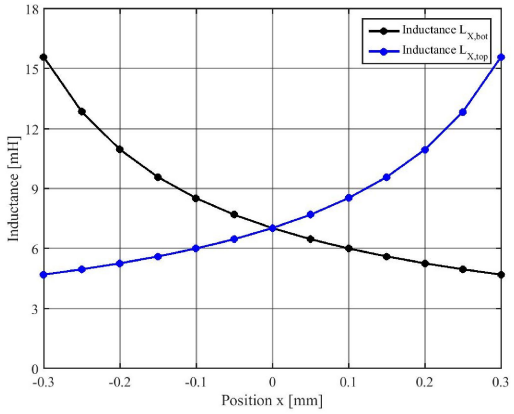

Figure 5. Simulated self-inductances $L_{X,top}$ and $L_{X,bot}$ of two opposite coils by FEA depending on the rotor position x at constant zero displacement y=0 and I_{bias}=0.

SELF-SENSING PRINCIPLE

For self-sensing AMBs the rotor position information is obtained by measuring the position-dependent coil inductances through electrical quantities such as currents (or current slopes) and voltages. Thus, the AMB works as actuator and sensing-unit simultaneously. Neglecting the ohmic voltage drop, induced voltages and possible inductance change rates per time due to rotor movements, the coil current $I_{X,top}$ fulfills

$$\frac{dI_{X,top}}{dt} = \frac{U_{DC}}{L_{X,top}}, \qquad (2)$$

where $L_{X,top}$ is the coil inductance and U_{DC} is the applied voltage from the H-bridge power amplifier during a positive switching state S_1=S_4=1 and S_2=S_3=0 (Fig. 6). Using the differential approach with two opposite coils in anti-parallel connection with inductances $L_{X,top}$ and $L_{X,bot}$ the common derivative of the current difference ΔI_X during a positive inverter switching state yields

$$\frac{d\Delta I_X}{dt} = \frac{dI_{X,top}}{dt} - \frac{dI_{X,bot}}{dt} = U_{DC}\left(\frac{1}{L_{X,top}} - \frac{1}{L_{X,bot}}\right). \qquad (3)$$

Herein, the difference of the inverse inductances contains the rotor position information. In Fig. 7 this term is evaluated with regard to the rotor position x for several control currents I_X. A continuous and nearly linear dependency on the rotor displacement x is given. At higher loads actuator saturation occurs and only leads to slight deviation from the linear behavior at high displacements. Because of the differential evaluation the mean values of the currents $I_{X,top}$ and $I_{X,bot}$ cancel each other. Thus, for slope detection the transformer can be small and still operates without saturation. The transformer for slope evaluation is implemented directly in the power electronics. Even a PCB integrated solution can be realized as in [5].

According to [4] the slope of the current difference $d\Delta I_X/dt$ can be evaluated by two different methods. Using the transformer as current transducer requires an additional resistor and at least two sample values to build the derivative. In contrast, by using an open-loop transformer the derivation operation is already included and the current slope can be detected by at least one sample of the induced voltage $U_{\Delta IX}$ at the transformer coil. Finally, this allows a slope detection within a short period during the pulse width modulation (PWM) cycle of the inverter. Therefore, the open-loop principle was chosen in this work.

For each axis, the appropriate coils are connected anti-parallel to a full H-bridge. The control current I_X is measured by shunt resistors at H-bridge low side transistors. By the anti-parallel winding connection, the control current I_X is split into two components $I_{X,top}$ and $I_{X,bot}$. By symmetrical switching of the H-bridge (S_1=S_4 and S_2=S_3) the voltage U_{DC} is applied alternating positive and negative to the anti - parallel coil.

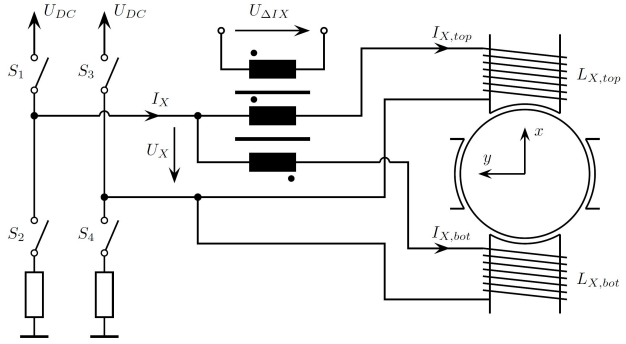

Figure 6. AMB system topology (simplified coils) for the x-axis; two opposite control coils for self-sensing based on the open-loop differential transformer principle, without bias coil.

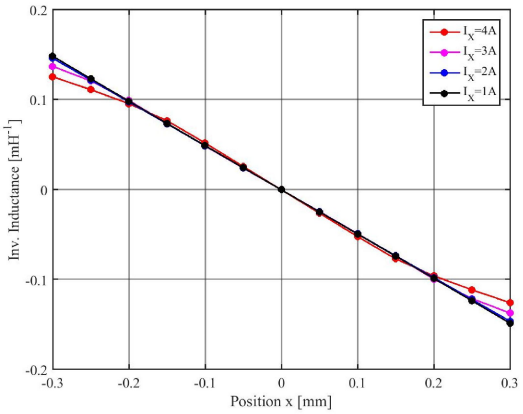

Figure 7. Differences of inverse inductances ($L_{X,top}^{-1}$-$L_{X,bot}^{-1}$) depending on the rotor position x at various control currents I_X at I_{bias}=0 and y=0.

Hence, these positive or negative voltages result in a nearly linear current slope with appropriate sign. The average current value I_X is set by the duty cycle of the positive and negative pulses at the PWM with constant frequency. The current signal contains a current ripple which on the one hand shall be low to ensure a low force ripple during operation, see Equ. (1). Further, the iron losses in the AMB stator are lower at low current ripples. On the other hand, a certain current ripple is required to allow a sensorless position estimation according to Equ. (3). Thus, from a system perspective a compromise has to be chosen for implementing self-sensing technology to AMBs.

A simulation for analyzing the current signal I_X and the current difference ΔI_X=$I_{X,top}$-$I_{X,bot}$ with applied voltages at U_{DC}=14V, f_{PWM}=20kHz is shown in Fig. 8. At centered position (x=0) both inductances $L_{X,top}$ and $L_{X,bot}$ are equal and the current difference ΔI_X is equal to zero. At a positive displacement x=0.3mm $L_{X,top}$ is high resulting in a small ripple of $I_{X,top}$. In contrast $L_{X,bot}$ is small, which leads to a high ripple of $I_{X,bot}$. Therefore, the resulting current difference ΔI_X has a negative slope at rising current $I_{X,top}$. During the time frame of applying negative voltage the slope of ΔI_X is negative. For a negative rotor position the slope of ΔI_X is positive. Because of the ohmic voltage drop of the coils for I_X=1A a positive average voltage at the bridge output U_X=(2δ-1)U_{DC} has to be applied resulting in a duty cycle δ>0.5. Further, this voltage drop leads to a slightly different slope at positive and negative applied voltage. This effect increases at lower DC voltages, because higher duty cycles are required to apply the average voltage U_X. To finally reach a high quality self-sensing the ohmic voltage drop has to be considered in the self-sensing algorithm.

The simulation has shown that utilizing this topology for self-sensing, a position information is included in the differential current during the positive as well as the negative switching state of the inverter. Evaluation of both slopes appropriately allows a very high self-sensing bandwidth of at least two slope samples per PWM period. Further, even duty cycle zero and one can be applied, which leads to a highly dynamic operation without any further voltage limitation for self-sensing. Because of the open loop transformer principle the differentiation operation is already integrated. Therefore,

only one single current slope sample of $U_{\Delta IX}$ is required. Thus, higher inverter switching frequencies are possible compared to derivative evaluation by two samples out of the current signal ΔI_X. This analysis by a 2D-FEA of the eight-pole AMB with differential winding topology confirms the fundamental working principle of the AMB as actuator as well as the possibility for self-sensing.

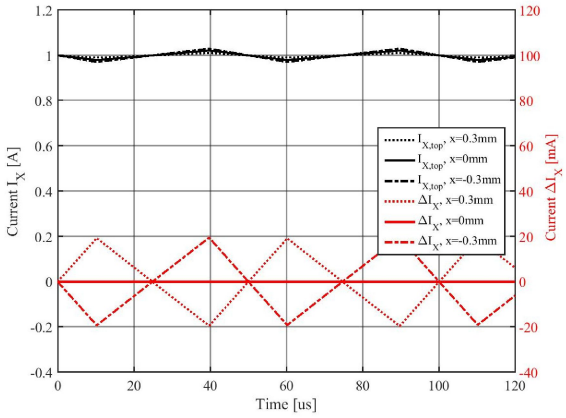

Figure 8. Coil current $I_{X,top}$=1A and current difference ΔI_X at various rotor displacements x, at I_{bias}=0, and y=0, f_{PWM}=20kHz and U_{DC}=14V.

Figure 9. Eight-pole AMB with bias coils for self-sensing control applied to a high speed synchronous reluctance machine.

Experimental Results

For experimental verification of the proposed AMB the prototype (Fig. 9) was built. A MOSFET inverter with three H-bridges is utilized for excitation of the control and bias coils. For a self-sensing rotor position analysis the inverter is equipped with a differential transformer (Fig. 6) for the x- as well as for the y-control coil. Two opposite coils are connected to one H-bridge. The coil currents I_X and I_Y are measured by the shunt resistors at the low side transistors within the inverter. Thus, at the AMB no sensing unit is required because both the current and differential transformer are integrated in the inverter. For current control and sensorless position detection a dual core signal processor TMS320F28377D is utilized. This high computational power allows flexibility in adjustment of the control algorithm with regard to self-sensing. This first prototype setup does not contain any external position sensors for comparison with self-sensing signals. Only the maximum eccentricity position at the safety bearing is used in this project phase.

As already known, the position dependency of the coil inductances is the key for self-sensing AMBs. Therefore, first the self-inductances according to Fig. 5 were measured at the AMB prototype for rotor displacements defined by the safety bearings. The bearing's magnetic airgap is 0.5mm and at displacements of 0.3mm the rotor touches the safety bearings. By experiments, the value $L_{X,top}$=20.1mH at a rotor position x=0.3mm and $L_{X,top}$=6.0mH at x=-0.3mm were identified. Both values are slightly higher than the simulated values, because of neglecting the leakage flux in the 2D simulation. However, this simple measurement verified the significant influence of the rotor displacement on the coil self-inductances.

A further analysis is done by inverter excitation of the AMB. Thus, the time behavior as well as current and current slope signals for the self-sensing algorithm based on Equ. (3) are analyzed. By the software algorithm all three bridges have synchronized clocking. This is advantageous for measurement of the transient analog signals at low crosstalk from other signal paths. As stated, a low DC-link voltage has direct influence on the self-sensing behavior. Therefore, a low DC-link voltage U_{DC}=14V was chosen to verify the proposed method with low current ripples. At f_{PWM}=20kHz, I_{bias}=0 and a duty cycle δ=0.5 the differential current ΔI_X and the induced transformer voltage $U_{\Delta IX}$ is evaluated (see Fig. 6). The voltage $U_{\Delta IX}$ is fed into an analog amplifier and shifted to positive values by an offset of 1.5V and further provided to the ADC (analog to digital converter) of the controller, see voltage U_{ADC} in Fig. 10 and Fig. 11. At a negative displacement x=-0.3mm and positive voltage (PWM signal in Fig. 10) the slope of ΔI_X is positive (blue) and results in a high positive voltage $U_{\Delta IX}$, respectively U_{ADC}>1.5V (red). In Fig. 11 the positive displacement x=0.3mm is depicted and results in the other signs of the signals ΔI_X and $U_{\Delta IX,}$ respectively U_{ADC}.

The inverter switching behavior results in a short oscillation of the current immediately after the switching event. Consequently, after a short settling time of approx. 7µs the current slope is identified at the voltage U_{ADC}. During the

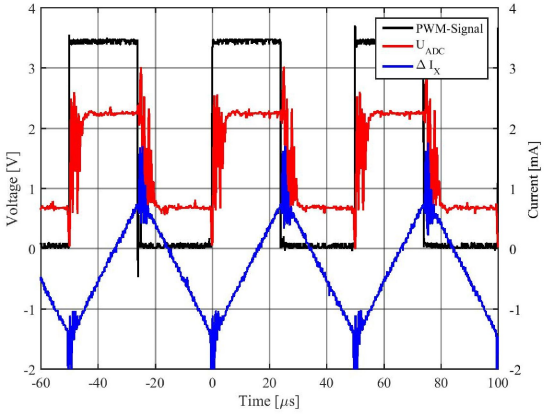

Figure 10. Measured signals (current difference ΔI_X and amplified transformer voltage U_{ADC}) for self-sensing rotor position detection in the x-axis at x=-0.3m, I_{bias}=0 and I_X=0.

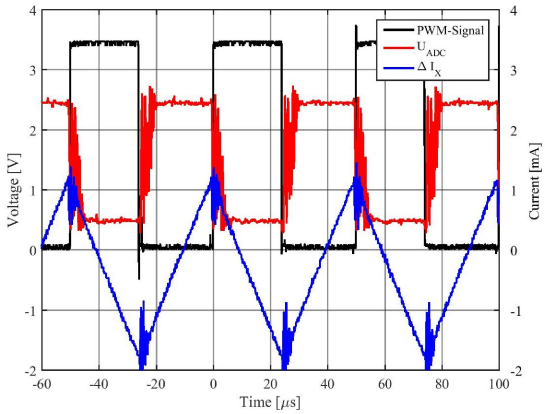

Figure 11. Measured signal for self-sensing rotor position detection in the *x*-axis signals for rotor position *x*=0.3mm, I_{bias}=0 and I_X=0.

time frame of constant voltage U_{ADC} one sample is taken at positive and negative voltages. Compared to the simulation the current difference is only approx. 2.7mA because of induced voltages from the bias coil. Therefore, the transformer winding ratio was adjusted for a high utilization of the analog input of the controller.

The rotor position by both axis is evaluated at constant eccentricity given by the airgap of the safety bearings (Fig. 12.). For constant eccentricity a circular shape is expected. The measured characteristic shows only a small deviation at I_{bias}=0 caused by the mechanical setup. Further, an increasing bias current leads to slight saturation at this high displacements and the circular shape is deformed in parts of the locus. A detailed analysis with comparison to external position sensors like in [6] is planned for future work.

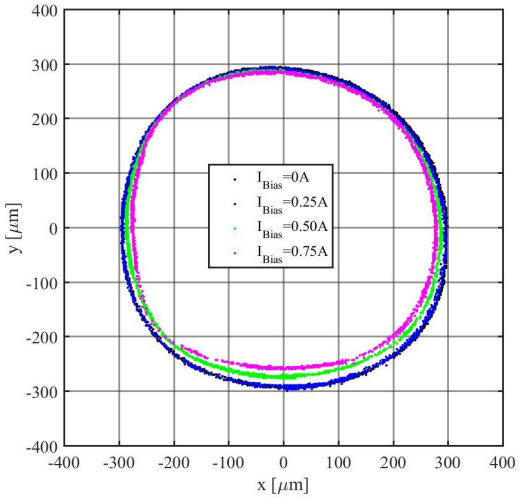

Figure 12. Sensorless rotor position at constant eccentricity of 0.3mm defined by contact to the safety bearing.

CONCLUSIONS

This work discusses the characteristics of a conventional eight-pole radial active magnetic bearing with a differential winding topology. By current biasing the bearing parameters can be varied in a certain range and adjusted to the application. A finite element analysis of the bearing was performed related to the force characteristic and the coil inductances. The coil inductance dependency on the rotor position is the basis for self-sensing. In this work a differential approach utilizing two opposite coils to one displacement signal by an open-loop transformer is proposed. The principle of sensorless rotor position detection is discussed also by simulations. An AMB prototype was built up and first experiments regarding to self-sensing were performed. Measured time sequences of appropriate signals for self-sensing explain the working principle and even the sensorless obtained position locus is presented. These first results confirm the possibility for a future self-sensing of the current biased radial AMB.

A full self-sensing levitation at this AMB was not investigated until now. To finally apply a closed loop control additional investigations are required. Further, for reference external position sensors have to be implemented. In this work several findings for a future self-sensing operation are already identified. Effects of induced voltages from the synchronously clocked bias coil as well as the ohmic voltage drop of the control coils have influence on the position sensing behavior. Cross-coupling of inductances and forces between the perpendicular axes affect the control during operation. Typically, for AMBs the saturation caused either by the excited coils or high displacements leads to nonlinearities with impact on the position accuracy. Eddy current effects, which are usually also limiting self-sensing, are covered by the differential approach. For an operation at centered rotor a detailed investigation on the small signal behavior, linearity, position accuracy and position noise is recommended. The dynamic behavior of the current control, the lift up behavior and optimization of the bearing losses by choosing the bias and control currents are further topics. Influence of the gyroscopic effect and rotor dynamic have to be also covered for applying this self-sensing approach to commercial AMB applications.

REFERENCES

[1] G. Schweitzer, “Magnetic Bearings, Theory, Design, and Application to Rotating Machinery”, Springer, Berlin, 2009

[2] E. Malsen, “Selfsensing for active magnetic bearings: overview and status”, *Proceedings of the Tenth International Symposium on Magnetic Bearings* (ISMB10), 2006

[3] M. Hofer, Th. Nenning, M. Hutterer, M. Schrödl, “Current Slope Measurement Strategies for Sensorless Control of a Three Phase Radial Active Magnetic Bearing”, *Proceedings of The 22nd International Conference on Magnetic Levitated Systems and Linear Drives*, MagLev 2014, Rio de Janeiro, Brazil, 28.09.2014 - 01.10.2014

[4] T. Nenning, M. Hofer, M. Hutterer, M. Schrödl, “Statistic Errors of Different INFORM Evaluation Methods Applied to Magnetic Bearings”, *Proceedings of the Fourteenth International Symposium onMagnetic Bearings* (ISMB14), Linz, 2014, pages 685-688

[5] M. Hofer, M. Hutterer, M. Schrödl, “PCB Integrated Differential Current Slope Measurement for Position-Sensorless Controlled Radial Active Magnetic Bearings”, *Proceedings of the 15th International Symposium on Magnetic Bearings* (ISMB15), Kitakyushu, Japan, August 3-6, 2016

[6] D. Wimmer, M. Hutterer, M. Hofer, M. Schrödl, “Variable Space Vector Modulation for Self-Sensing Magnetic Bearings”, *Proceedings of the 16th International Symposium on Magnetic Bearings* (ISMB16), Beijing, China, August 13-17, 2018